Quantum-Well Infrared Phototransistor With pHEMT Structure

Joon Ho Oum, Uk Hyun Lee, Yong Hoon Kang, Jong Ryul Yang, and Songcheol Hong, *Member, IEEE*

***Abstract*—A quantum-well infrared phototransistor with a pseudomorphic high-electron mobility transistor (pHEMT) structure is presented. The proposed phototransistor uses four periods of a $\mathrm{GaAs/Al_{0.3}Ga_{0.7}As}$ (50 Å/120 Å) quantum-well absorption region, as well as an $\mathrm{In_{0.15}Ga_{0.85}As}$ quantum well conducting channel under the absorption layer. The phototransistor shows a large responsivity of 140 A/W around 6 μm at 23 K (for a cutoff wavelength of 7.5 μm). The relation between the photoconductive gain and the transconductance of the pHEMT structure is also investigated.**

***Index Terms*—Infrared (IR) detectors, MODFETs, quantum-well (QW) devices, quantum-well infrared photodetectors (QWIPs).**

I. INTRODUCTION

INFRARED (IR) imaging systems have been widely used in various fields of applications, including industrial, defense, security, and medical applications, and IR photodetectors are key elements of IR imaging systems. The medum-wavelength IR (MWIR, 3 to 5 μm) and long-wavelength IR (LWIR, 8 to 14 μm) are interesting wavelength range for IR detectors. This is because the ranges of MWIR and LWIR are atmospheric windows in which the IR light can propagate a long distance with low air absorption. Many researchers have widely investigated quantum structure IR photodetectors that use the intersubband transitions of quantum-wells (QWs) or quantum dots because, compared to detectors that use materials with a small energy bandgap, such as HgCdTe (MCT) and InSb, quantum structure IR photodetectors have easy wavelength tunability and can be operated at high temperature [1], [2]. Moreover, quantum-well IR photodetectors (QWIPs) can be used as the focal plane arrays of an IR imaging camera [3].

Typically, QWIPs use the conventional n-i-n photodiode structure and have low photoconductive gains. The responsivity (R) of a typical QWIP (with the n-i-n photodiode structure) is proportional to the product of the quantum efficiency (η) and the photoconductive gain (g), as shown as follows in (1):

$$\mathrm{R} = \eta \frac{e}{\mathrm{hv}} g. \tag{1}$$

In typical QWIPs, η and g cannot be increased at the same time because the number of absorption layers (which increase η) increases the length of the photo-excited electrons path, thereby decreasing the photoconductive gain. Thus, typical QWIPs have a similar level of responsivity ($\sim$1 A/W) regardless of the QW periods [4], [5]. For focal plane arrays, typical QWIPs use CMOS address switches to get an output signal from an addressed pixel, and the switches are integrated into a read-out integrated circuit. Aside from allowing high responsivity, the proposed QWIP with the pHEMT structure obviates the need for the CMOS address switches and enables the read-out integrated circuit to be simplified because a gate can be used as the devices switch.

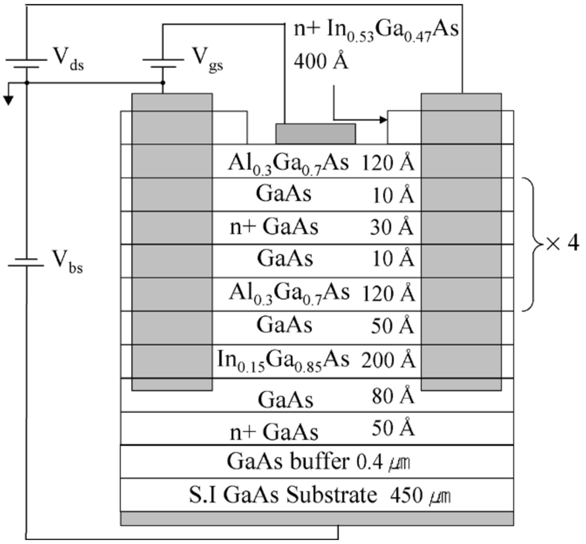

Fig. 1. Structure of the proposed QWIP-pHEMT with the electrodes and bias notations.

Cho and Lee reported on lateral quantum dot IR photodetectors (QDIPs)that have a high degree of responsivity and can be operated at high temperatures [6], [7]. However, these QDIPs do not have pHEMT structure but a pHEMT-epi structure, which basically comprises two terminal devices and a laterally transporting channel. The lateral structure has not yet been applied to QWIPs; furthermore, there have been no reports on QWIPs with a pHEMT structure. We therefore introduce a QWIP with a pHEMT structure and explain the mechanism of its large degree of responsivity.

II. DEVICE STRUCTURE AND FABRICATION

Fig. 1 shows an epitaxial structure of a QWIP with a pHEMT structure. The absorption layer consists of four periods of $\mathrm{GaAs/Al_{0.3}Ga_{0.7}As}$ (50 Å/120 Å) QWs, in which each conduction band was designed to have only one bound

Manuscript received March 23, 2005; revised May 10, 2005. This work was supported in part by KISTEP under the Nano-Structure Technology Projects and the donation support program of the IMT2000 R&D and in part by the MOE BK21 program. The review of this letter was arranged by Editor D. Ritter.

The authors are with the Department of Electrical Engineering and Computer Science, Korea Advanced Institute of Science and Technology, Daejeon 305-701, Korea (e-mail: penrose@kaist.ac.kr).

Digital Object Identifier 10.1109/LED.2005.852539

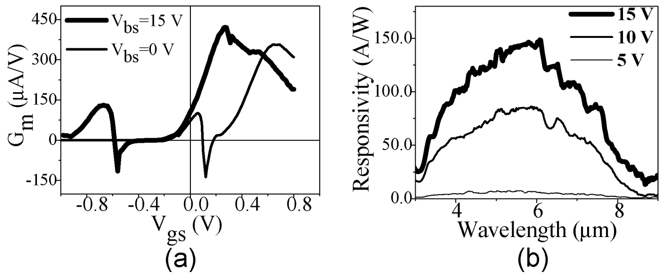

Fig. 2. (a) Measured transconductance G_m $(= \Delta I_{\rm ds}/\Delta V_{\rm gs})$ when $V_{\rm bs} =$ 0 V and 15 V at 23 K and $V_{\rm ds} = 4$ V. (b) Responsivity spectra with different back-gate voltages ($V_{\rm bs} = 5$ V, 10 V, 15 V) at 23 K and $V_{\rm ds} = 4$ V.

state. We doped the center of the GaAs well (30 Å thick) at $n = 1 \times 10^{18}$ cm^{-3} to supply electrons to the QWs. When the IR light is incident to the QWs and absorbed, the electrons in the QWs had bound-to-continuum transitions. Then the photo-excited electrons are collected to $\rm In_{0.15}Ga_{0.85}As$ layer (channel) and transport along drain and source contacts. The 50 Å n-doped $(1 \times 10^{18}$ cm$^{-3})$ GaAs layer under the channel, which had an 80 Å undoped GaAs spacer, also supplies electrons to the $\rm In_{0.15}Ga_{0.85}As$ channel.

For drain and source contacts, we deposited and annealed AuGe/Ni/Au on the $\rm In_{0.53}Ga_{0.47}As$ (400 Å, n-doped 5×10^{18} cm^{-3}) layer. A succinic acid solution was used to selectively etch the $\rm In_{0.53}Ga_{0.47}As$ layer onto the $\rm Al_{0.3}Ga_{0.7}As$ layer. After a device isolation step, we deposited Ti/Pt/Au on the $\rm Al_{0.3}Ga_{0.7}As$ layer to make the gate, and then deposited back-gate metal (Au) on the substrate after polishing the 45° parallel facets at the end of the sample. Because the n-type QWIP uses intersubband transitions in the conduction band, this QWIP does not respond to normal incidence IR light, because of the well-known selection rule of the intersubband transitions in QWs. Thus, the detector must have a light coupler with a 45° polished facet that converts light that is normally incident to laterally traveling light. We made two QWIPs, each with a pHEMT structure and a different window area (50 × 33 μm; 50 × 25 μm), and we verified that the photocurrents are proportional to the device areas.

III. RESULTS AND DISCUSSION

Fig. 2(a) shows the $G_m (= \Delta I_{\rm ds}/\Delta V_{\rm gs})$ characteristics of the pHEMT structure at 23 K. At room temperature, a QWIP with the pHEMT structure has typical current–voltage (*I–V*) characteristics. However, at low temperature, the *I–V* characteristics of a QWIP with the pHEMT structure collapse due to the electron trapping in the QW layers when positive gate voltages $(V_{\rm gs} > 0)$ are applied. This collapse accounts for the dip at $V_{\rm gs} = 0.12$ V in the G_m, which is shown in Fig. 2(a). The electron trapping effect at low temperature has also been reported in an AlGaAs/GaAs high electron mobility transistor (HEMT) [8].

Because we used a QWIP with a pHEMT structure as a photodetector, the gate voltage had to be set to negative $(V_{\rm gs} < 0)$ so that the photo-excited electrons were readily collected in the $\rm In_{0.15}Ga_{0.85}As$ channel. When the gate voltage became negative, the density of two-dimensional electron gas (2DEG) in the channel decreased and the QW was finally depleted. We therefore applied a positive voltage on the back-gate to keep the density of 2DEG sufficient to have a gain in the channel current and associated transconductance. Furthermore, as shown in Fig. 2(a), the threshold gate voltage decreased when we applied the positive back-gate voltage.

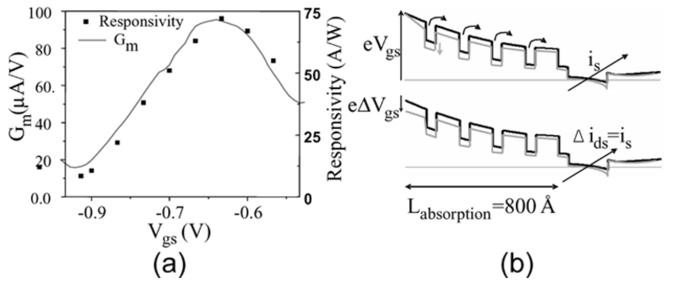

Fig. 3. (a) Gate bias dependence of G_m $(= \Delta I_{\rm ds}/\Delta V_{\rm gs})$ and the measured peak responsivities at 6 μm at 23 K ($V_{\rm bs} = 10$ V, $V_{\rm ds} = 4$ V). (b) Energy band diagram of the QWIP with the pHEMT structure. Each bright line represents the band diagram when the QWIP is under illumination (up) and gate voltage is increased by $\Delta V_{\rm gs} (> 0)$ in the dark condition (down).

Fig. 2(b) shows the calibrated responsivity spectra of the QWIP with the pHEMT structure at different back-gate biases at 23 K ($V_{\rm ds} = 4$ V, $V_{\rm gs} = -0.65$ V, $V_{\rm bs} = 15$ V). To measure the photocurrent spectra, we used a grating-monochromator, optical filters, a low noise current amplifier, and a lock-in amplifier with an optical chopper. We then obtained the responsivity spectra from the photocurrent spectra of the QWIP and from a standard MCT detector whose responsivity spectrum was well known. The cutoff wavelength was 7.5 μm. In addition, the maximum peak responsivity was 140 A/W when $V_{\rm bs} = 15$ V and 5 A/W when $V_{\rm bs} = 5$ V (at 6 μm). The responsivity of 140 A/W is a hundred times greater than the responsivity of a conventional n-i-n vertical diode-type QWIP and this level was maintained up to 53 K.

Fig. 3(a) shows the relation of G_m and the peak responsivity at 6 μm ($V_{\rm ds} = 4$ V, $V_{\rm bs} = 10$ V, at 23 K). Note that the peak responsivity curve follows the G_m curve. We can estimate the gain of the QWIP with the pHEMT structure from the G_m and the photocurrent. The photoconductive gain from the QWIP itself, as in a conventional n-i-n diode structure, is negligible because the gain from the pHEMT structure is enormous. In Fig. 3(b), the photo-excited electrons from the QWs move to the channel and are transported along the channel by the lateral field of the drain/source, thereby increasing the density of 2DEG in the channel. This increase is equivalent to the increment of the gate voltage $(\Delta V_{\rm gs} > 0)$ of the pHEMT. If the IR light is incident to the QWs whose flux density (the number of photons per unit area and per second) is Φ_s, the number (n_i) of electrons generated from the $i_{\rm th}$ QW can be written as $n_i = \eta_i A_d \Phi_s$, where η_i is the quantum efficiency (η_i) of the $i_{\rm th}$ QW. When electrons escape from the QWs, the net charge of the QWs becomes positive as a result of Δq. We therefore assume that Δq can be written by using the value of n_i as follows:

$$\Delta q = e\, A_d\, \eta_i \Phi_s. \tag{2}$$

Assuming that a QWIP with a pHEMT structure has only the gain of the pHEMT structure, the photocurrent and responsivity of the QWIP with the pHEMT structure can be written as

$$\begin{aligned} i_s &= G_m \Delta V_{\mathrm{gs}} \\ &\approx G_m \left(\frac{\mathrm{eA}_d \Phi_s}{2\varepsilon_s} \sum_i \eta_i \right) L_{\mathrm{absorption}} \\ &= \frac{\mathrm{eA}_d \Phi_s L_{\mathrm{absorption}}}{2\varepsilon_s} G_m \eta \end{aligned} \tag{3}$$

$$\begin{aligned} \mathrm{R} &= \frac{i_s}{A_d \Phi_s \mathrm{hv}} \\ &= \eta \frac{e}{\mathrm{hv}} \frac{G_m L_{\mathrm{absorption}}}{2\varepsilon_s} \\ &= \eta \frac{e}{\mathrm{hv}} g_{\mathrm{QWIP-pHEMT}} \end{aligned} \tag{4}$$

where ΔV_{gs}, is the equivalent gate voltage increment in a dark condition, that makes the I_{ds} increment equals to the photocurrent under illumination, as shown in Fig. 3(b). The $L_{\mathrm{absorption}}$ parameter is the length of the absorption layer (800 Å), ε_s is the dielectric constant of $\mathrm{Al_{0.3}Ga_{0.7}As}$, $\eta(=\sum_i \eta_i)$ is the total quantum efficiency of four periods of the QWs, $\mathrm{h}\nu$ is the energy of a single photon, and $g_{\mathrm{QWIP-pHEMT}}$ is the gain of the QWIP with the pHEMT structure.

To measure the IR flux density, we used the photocurrent and responsivity of a standard MCT detector by the relation $i_{\mathrm{sMCT}} = A_{\mathrm{dMCT}} \Phi_s h\nu R_{\mathrm{MCT}}$. Here, i_{sMCT} is the photocurrent, A_{dMCT} is the window area of the detector, and R_{MCT} is the responsivity of the standard MCT detector. In our measurement system and device, the measured photocurrent was 13.5 nA and the IR flux density at a wavelength of 7.5 μm was $4.99 \times 10^{14}\ s^{-1}\mathrm{cm}^{-2}$ when $V_{\mathrm{bs}} = 15$ V, $V_{\mathrm{gs}} = -0.65$ V, and $V_{\mathrm{ds}} = 4$ V, $A_d = 50 \times 25\ \mu\mathrm{m}^2$ and $G_m = 1.28 \times 10^{-4}$ A/V. Using these parameters, we calculated the quantum efficiency for the four periods of the QW layers and obtained values of $\eta = 2.85\%$ and $g_{\mathrm{QWIP-pHEMT}} = 474$. This estimated quantum efficiency is a reasonable value because the efficiency for 25 periods of an $\mathrm{Al_{0.3}Ga_{0.7}As/GaAs}$ (50 Å/50 Å) QWIP at 7.5 μm was about 20% [9]. We deduce, therefore, that the large responsivity originates from the large G_m of the pHEMT structure.

The detectivity, which represents the signal-to-noise ratio of the detector, was $2.4 \times 10^{10}\ \mathrm{cm} \cdot \mathrm{Hz}^{1/2}/\mathrm{W}$ (6 μm, 23 K), and the maximum operating temperature was 65 K. The detectivity is smaller by one order than 50 periods of a typical AlGaAs/GaAs QWIP ($\eta = 16\%$, maximum detectivity$= 2 \times 10^{11}\ \mathrm{cm} \cdot \mathrm{Hz}^{1/2}/\mathrm{W}$) because of small quantum efficiency of QWIP-pHEMT ($\eta = 2.85\%$) [3]. However, the quantum efficiency can be improved sufficiently by increasing the number of periods of the QWs and by using light coupling structures. As a result, we can implement focal plane arrays that use the QWIP with the pHEMT structure without a CMOS switch, thereby simplifying the readout circuits. In this letter, optimum operating gate voltage of QWIP-pHEMT is -0.65 V, therefore the device can be turned on by applying -0.65 V to the gate and turned off ($I_{\mathrm{ds}} = 0$) by setting the gate voltage below the pinch off.

IV. CONCLUSION

We have demonstrated a QWIP with a pHEMT structure, and shown it to have a responsivity that is a hundred times larger than that of a typical QWIP. This large responsivity (140 A/W) is due to the transconductance (G_m) gain of the pHEMT structure. However, even though the QWIP with the pHEMT structure has a larger degree of responsivity than typical QWIPs, the signal-to-noise ratio is not improved because the quantum efficiency is small and the electrons that escape from the QW by thermal emission are amplified by the transconductance of the pHEMT structure.

REFERENCES

[1] B. F. Levine, C. G. Bethea, G. Hasnain, J. Walker, and R. J. Malik, "High-detectivity $D^* = 1.0 \times 10^{10}$ cmHz$^{1/2}$W GaAs/AlGaAs multiquantum-well $\lambda = 8.3\ \mu$m infrared detector," *Appl. Phys. Lett.*, vol. 53, pp. 296–298, May 1988.

[2] S. Chakrabarti, A. D. Stiff-Roberts, P. Bhattacharya, S. Gunapala, S. Bandara, S. B. Rafol, and S. W. Kennerly, "High-temperature operation of InAs-GaAs quantum-dot infrared photodetectors with large responsivity and detectivity," *IEEE Photon. Technol. Lett.*, vol. 16, no. 5, pp. 1361–1363, May 2004.

[3] S. D. Gunapala, S. V. Bandara, J. K. Liu, E. M. Luong, N. Stetson, C. A. Shott, J. J. Bock, S. B. Rafol, J. M. Mumolo, and M. J. McKelvey, "Long-wavelength 256 × 256 GaAs/AlGaAs quantum-well infrared photodetector (QWIP) palm-size camera," *IEEE Trans. Electron Devices*, vol. 47, no. 2, pp. 326–332, Feb. 2000.

[4] K. M. S. V. Bandara, B. F. Levine, and M. T. Asom, "Tunneling emitter undoped quantum-well infrared photodetector," *J. Appl. Phys.*, vol. 74, no. 1, pp. 346–350, Jul. 1993.

[5] S. D. Gunapala, B. F. Levine, and N. Chand, "Bound to continuum superlattice miniband long wavelength GaAs/$\mathrm{Al}_x\mathrm{Ga}_{1-x}\mathrm{As}$ photoconductors," *J. Appl. Phys.*, vol. 70, no. 1, pp. 305–308, Jul. 1991.

[6] T. Cho, J. W. Kim, J. E. Oh, J. W. Choe, and S. Hong, "A long-wavelength infrared photodetector with self-organized InAs quantum dots embedded on HEMT-like structure," *Jpn. J. Appl. Phys.*, pt. 1, vol. 38, no. 4B, pp. 2442–2444, Apr. 1999.

[7] S. W. Lee, K. Hirakawa, and Y. Shimada, "Bound-to-continuum intersubband photoconductivity of self-assembled InAs quantum dots in modulation-doped heterostructures," *Appl. Phys. Lett.*, vol. 75, pp. 1428–1430, 1999.

[8] A. Kastalsky and R. A. Kiehl, "On the low-temperature degradation of (AlGa)As/GaAs modulation-doped field-effect transistors," *IEEE Trans. Electron Devices*, vol. 33, no. 3, pp. 414–423, Mar. 1986.

[9] S. D. Gunapala and K. M. S. V. Bandara, "Homojunction and quantum-well infrared detectors," in *Thin Films*, M. H. Francombe, Ed. New York: Academic, 1995, vol. 21, pp. 144–146.